Published in final edited form as:
Nat Neurosci. ; 15(8): 1153–1159. doi:10.1038/nn.3166.

Dissecting Spatial Knowledge from Spatial Choice by Hippocampal NMDA Receptor Deletion

David M. Bannerman[1,*], **Thorsten Bus**[2], **Amy Taylor**[1], **David J. Sanderson**[1], **Inna Schwarz**[2], **Vidar Jensen**[3], **Øivind Hvalby**[3], **J. Nicholas P. Rawlins**[1], **Peter H. Seeburg**[2,*], and **Rolf Sprengel**[2]

[1]Department of Experimental Psychology, University of Oxford, Oxford OX1 3UD, U.K.

[2]Max Planck Institute for Medical Research, D-69120 Heidelberg, Germany

[3]Department of Physiology, Institute of Basic Medical Sciences, University of Oslo, N-0317 Oslo, Norway

Abstract

Hippocampal NMDA receptors (NMDARs) and NMDAR-dependent synaptic plasticity are widely considered as crucial substrates of long-term spatial memory, although their precise role remains uncertain. Here we show that *GluN1*$^{\Delta DGCA1}$ mice, lacking NMDARs in all dentate gyrus and dorsal CA1 principal cells, acquired the spatial reference memory watermaze task as well as Controls, despite impairments on the spatial reference memory radial maze task. In a novel spatial discrimination watermaze paradigm, using two visually identical beacons, *GluN1*$^{\Delta DGCA1}$ mice were impaired at using spatial information to inhibit selecting the decoy beacon, despite knowing the platform's actual spatial location. This failure could suffice to impair radial maze performance despite spatial memory itself being normal. Thus, these hippocampal NMDARs are not essential for encoding or storing long-term, associative spatial memories. Instead, we demonstrate an important role for the hippocampus in using spatial knowledge to select between alternative responses that arise from competing or overlapping memories.

The ability to associate spatial locations with particular events is essential for the survival of all animals. It is widely believed that NMDAR-dependent synaptic plasticity contributes to the formation of associative memories[1], and hippocampal NMDARs, particularly those in the dorsal CA1, are thought to be important for associative, long-term spatial memory[2], although their precise role remains unclear. Indeed, as recently noted, "even though the synaptic plasticity and memory hypothesis is enshrined in most neuroscience text books, this issue is still far from resolved"[3]. Pharmacological studies with NMDAR antagonists are equivocal[4-6], and previous evidence from transgenic mice lacking NMDARs in dorsal

[*]Correspondence: David.Bannerman@psy.ox.ac.uk, Phone: 0044-1865271426 Fax: 0044-1865310447 and Peter.Seeburg@mpimf-heidelberg.mpg.de, Phone: 0049-6221486495 Fax: 0049-6221486110 .

methods Methods and any associated references are available in the online version of the paper at http://www.nature.com/neuroscience

Accession Codes. (MGI database, *Grin1*^{tm1Rsp} and *Gt(Rosa)26Sor*; Genotyping, see http://wmn.mpimf-heidelberg.mpg.de/sprengel.

Note: Supplementary information is available on the Nature Neuroscience website.

Author Contributions T.B., I.S. and R.S generated and molecularly analyzed the *GluN1*$^{\Delta DGCA1}$ mice. Ø.H and V.J. performed the electrophysiological analysis. D.B designed the behavioral experiments. D.B., D.S., and A.T. performed behavioral analyses. D.B., T.B., R.S., N.R. and P.S. wrote the manuscript.

Competing financial interest The authors declare no competing financial interests.

Europe PMC Funders Author Manuscripts

CA1[7,8] is confounded by the spread of NMDAR deletion to principal neurons in cortex, as evidenced in recent studies employing this transgenic line[9-13].

Mice lacking NMDARs selectively in dentate gyrus (DG) granule cells, and hence long-term potentiation (LTP) in lateral and medial perforant path synapses, exhibit normal long-term spatial memory[14,15]. We have now generated mice (*GluN1*$^{\Delta DGCA1}$) in which NMDARs are additionally lacking in dorsal and, to a lesser extent, ventral hippocampal CA1 pyramidal cells, specifically in adulthood, thus providing an important new mouse model for assessing the hippocampal NMDAR and memory hypothesis. Here we investigated *GluN1*$^{\Delta DGCA1}$ mice on tests of associative long-term spatial memory. Mice were assessed on reference memory versions of the watermaze and radial maze tasks, which both depend on dorsal hippocampus[16-21].

RESULTS

DG and CA1 specific NMDAR deletion in *GluN1*$^{\Delta DGCA1}$ mice

We employed a mouse line (*GluN1*$^{\Delta DGCA1}$, Fig. 1a) gene-targeted for loxP-tagged *Grin1* alleles and carrying two transgenes *Tg*^{LC1} and *Tg*^{CN12}, which enabled doxycycline (dox)-sensitive, Cre-mediated GluN1 ablation in excitatory hippocampal, but not cortical, neurons of adults[22,23] by use of a CaMKII promoter fused to a *Grin2c* silencer element[24]. Selective hippocampal NMDAR removal required switching off Cre expression by dox during embryogenesis and nursing pups with mothers taken off dox post-natally. Delayed Cre expression, detected four weeks post-natally (Fig. 1b,c), eventually reached a peak in all DG granule cells, whereas in CA1, a Cre expression gradient formed along the dorso-ventral axis (Fig. 1d, Supplementary Fig. 1h). Specificity of cumulative Cre expression was assessed by X-gal staining in double transgenic Cre indicator mice (*Tg*$^{CN12/LC1}$/*Gt*(*Rosa*)*26Sor*) which demonstrated strong Cre-induced β-galactosidase activity throughout the entire DG and mossy fibers, as well as dorsal and, to a lesser extent, ventral CA1 (Fig. 1b,c, Supplementary Fig. 1d-g). All other parts of the hippocampal formation (CA3, lEnt, mEnt, Sub) exhibited negligible recombination (<1% co-labeling; Supplementary Fig. 1d-g), although β-galactosidase was observed in olfactory bulb granule cells and approximately 30% of layer II piriform cortex neurons (Fig. 1b,c, Supplementary Fig. 1d).

Efficient loss of GluN1 expression in dorsal CA1 and DG was confirmed by *in situ* hybridization, which also revealed reduced expression of the AMPAR subunit GluA1 in the DG granule cell layer (Fig. 1e, Supplementary Fig. 2). Further analysis indicated that in older mice the volume of the DG was reduced (~50% at age >P365). NeuN, Calbindin, GFAP and Parvalbumin expression patterns showed that the upper plate of the DG granule cell layer was more compromised than the lower plate, exhibiting gliosis in one-year old mice (Fig. 1f, Supplementary Fig. 3). Thus, chronic removal of NMDARs in these hippocampal areas resulted in thinning of the stratum granulare in DG, which might, in part, be related to a recently delineated role for NMDARs in the adult DG[25].

GluN1$^{\Delta DGCA1}$ mice appeared normal and were visually indistinguishable from their littermate controls. However, they were hyperactive when placed in a novel environment (Supplementary Fig. 4).

Electrophysiological analysis

As expected, no NMDAR-mediated responses could be evoked at CA3-to-CA1 synapses in dorsal hippocampal slices from adult *GluN1*$^{\Delta DGCA1}$ mice (Fig. 2a).

Extracellular field LTP experiments confirmed the loss of functional NMDARs in the Schaffer collateral/commissural pathway in dorsal CA1. In *GluN1*$^{\Delta DGCA1}$ mice, LTP failed to develop after four tetanizations (Fig. 2b).

In subsequent experiments, a stimulation electrode was placed in stratum radiatum, at the border between CA1 and CA3. Stimulation at 0.1 Hz elicited synaptic responses recorded simultaneously by two glass electrodes localized to stratum radiatum in CA1 and CA3. In Controls LTP was simultaneously well developed in both pathways 40–45 min after repeated tetanization, with a similar magnitude in the two subfields (Fig. 2c, upper panel). In *GluN1*$^{\Delta DGCA1}$ mice LTP in the CA3 subfield was preserved, whereas CA3-to-CA1 LTP was absent (Fig. 2c, lower panel), providing direct evidence for loss of NMDAR-mediated function in CA1. Thus, *GluN1*$^{\Delta DGCA1}$ mice provide a novel means of assessing the hippocampal NMDAR-dependent synaptic plasticity and memory hypothesis. Associative, long-term spatial memory was therefore assessed in *GluN1*$^{\Delta DGCA1}$ mice using two classic, hippocampus-dependent tests (Supplementary Fig. 5).

Spatial reference memory in the Morris watermaze

Mice with hippocampal lesions are unable to acquire the fixed location, hidden platform version of the watermaze (Supplementary Fig. 5a-c). In contrast, experimentally naïve *GluN1*$^{\Delta DGCA1}$ mice learned the spatial location of the platform as well as Controls (Fig. 3). Mice exhibited reduced pathlengths to find the platform as training proceeded but there was no impairment in *GluN1*$^{\Delta DGCA1}$ mice (ANOVA; main effect of block - $F(8,176) = 62.68$; $p < 0.0001$; no main effect of genotype - $F < 1$; no genotype by block interaction - $F(8,176) = 1.64$; $p > 0.10$; Fig. 3a, **Acquisition**). During probe tests in which the platform was removed from the pool, hippocampal lesioned mice characteristically searched equally across all four quadrants of the pool (Supplementary Fig. 5c), but in the first probe test (24 h after trial 24) both Controls and *GluN1*$^{\Delta DGCA1}$ mice exhibited strong spatial memory and searched selectively at the training platform location (Fig. 3b). ANOVA revealed only a significant main effect of quadrant ($F(2,66) = 49.66$; $p < 0.05$). In the second probe test (24 h after trial 36), *GluN1*$^{\Delta DGCA1}$ mice showed stronger spatial memory, and spent significantly more time in the training quadrant than Controls (Fig. 3c). ANOVA revealed a main effect of quadrant ($F(2,66) = 68.74$; $p < 0.05$), and a genotype by quadrant interaction ($F(2,66) = 3.27$; $p < 0.05$). There was a significant group difference in time spent in the training quadrant (t-test; $t(22) = 2.24$; $p < 0.05$).

On the next day the platform was moved to the opposite quadrant of the pool for a further 3 days of training. Whereas initial acquisition had been normal in *GluN1*$^{\Delta DGCA1}$ mice, during reversal learning they were significantly impaired, taking longer paths to the new platform position (ANOVA; main effect of genotype - $F(1,22) = 13.41$; $p < 0.005$; main effect of block - $F(2,44) = 36.54$; $p < 0.0001$; no genotype by block interaction - $F(2,44) = 2.24$; $p > 0.10$; Fig. 3a, **Reversal**).

Spatial reference memory on the radial maze

Although *GluN1*$^{\Delta DGCA1}$ mice displayed normal acquisition in the watermaze, they were, like mice with hippocampal lesions (Supplementary Fig. 5d), substantially impaired on acquisition of a radial maze task, in which they had to discriminate between three always-baited arms and three never-baited arms (Fig. 4). *GluN1*$^{\Delta DGCA1}$ mice made more reference memory errors (ANOVA; main effect of genotype - $F(1,21) = 30.42$; $p < 0.0001$; main effect of block - $F(11,231) = 16.08$; $p < 0.0001$; no genotype by block interaction - $F(11,231) = 1.03$; $p > 0.40$; Fig. 4a). The number of errors into the single, non-rewarded arm and the pair of adjacent, non-rewarded arms (allowing for the number of arms) were also compared (Fig. 4b). Mice were more likely to make errors into the single, non-rewarded arm than into one

of the adjacent, non-rewarded arms (ANOVA; main effect of error type – $F(1,21) = 7.06$; $p < 0.02$). However, this pattern was the same for both genotypes (genotype x error type interaction – $F < 1$; $p > 0.90$).

The dissociation between these two classic spatial reference memory tests (watermaze vs. radial maze) did not reflect differences in sensorimotor, motivational or arousal demands of these tasks[26]. The behavioral difference between genotypes was also present in both appetitive and aversive (swim/escape) versions of a three-arm radial maze (Y-maze) reference memory task. In both versions of this Y-maze task *GluN1*$^{\Delta DGCA1}$ mice were impaired during acquisition (Supplementary Fig. 6). Furthermore, both groups acquired an appetitively-motivated, visual discrimination task (grey vs. black/white striped goal arms) at a comparable rate (Fig. 5). ANOVA revealed a main effect of block ($F(8,176) = 36.18$; $p < 0.0001$), but no main effect of genotype ($F < 1$), and no genotype by block interaction ($F(8,176) = 1.07$; $p > 0.30$). They were also indistinguishable during subsequent reversal of this non-spatial task (Supplementary Fig. 7).

Spatial discrimination using a beacon watermaze task

Instead, the dissociation likely reflects the different psychological processes involved in these watermaze and radial maze tasks. On the radial maze, all arms have the same physical appearance (the intramaze cues are constant). They have the same Perspex door, the same grey floor and sidewalls, and the same foodwell. When mice find food at the ends of the arms these common features become associated with reward, so mice will tend to run down arms expecting food. However, these common intramaze cues are present in both rewarded and non-rewarded arms, and are therefore ambiguous. In order to inhibit the tendency to run down non-rewarded arms, and so discriminate successfully between baited and never-baited arms, the mice must therefore use the arm-specific, extra-maze spatial cues to select the correct response (run vs. don't run) for each arm. We hypothesized that it is this ability to use spatial information to disambiguate between competing or overlapping memories (a form of pattern separation), and thereby behaviorally inhibit inappropriate associative, conditioned responses that is impaired in *GluN1*$^{\Delta DGCA1}$ mice on this task.

To test this possibility, we trained experimentally naïve mice on a watermaze paradigm in which they were required to discriminate between two visibly identical beacons (black spheres), depending on their spatial locations (Fig. 6a)[27, 28]. One beacon was located over the platform. The other, "decoy" beacon was at the point-symmetrically opposite location in the pool and provided no escape. Both beacons remained in fixed spatial locations. Mice were placed into the pool, either close to the correct beacon (S^+ position), close to the decoy beacon (S^- position), or equidistant between the two beacons (Fig. 6b).

GluN1$^{\Delta DGCA1}$ mice were impaired in their spatial choices between the two beacons, despite knowing the platform's spatial location. During pre-training with a single beacon in a variable spatial location, all mice rapidly learned to swim towards the beacon and escape onto the platform. During subsequent spatial discrimination training both groups then learned to select the correct beacon according to its spatial location as shown by the gradual improvement in first choice accuracy (ANOVA; main effect of block - $F(4,84) = 24.52$; $p < 0.0001$; no main effect of genotype - $F(1,21) = 2.88$; $p > 0.10$; no genotype by block interaction - $F < 1$; $p > 0.70$; Fig. 6c). Furthermore, when probe tests were performed, with both beacons and the platform removed from the pool, both groups equally preferred the quadrant where the platform had been, demonstrating spatial learning (Fig. 6d; probe test 1 ANOVA; effect of quadrant - $F(2,63) = 19.29$; $p < 0.05$; no genotype by quadrant interaction - $F < 1$; $p > 0.80$; time spent in the training quadrant only – t-test; $t < 1$; $p > 0.80$; probe test 2 ANOVA; main effect of quadrant - $F(2,63) = 19.90$; $p < 0.05$; no genotype by quadrant interaction - $F(2,63) = 2.07$; $p > 0.10$; comparison of training quadrant times – t-

test; t (21) = 1.75; p = 0.09). Thus, *GluN1*$^{\Delta DGCA1}$ mice learned the location of the platform as well as the Controls, successfully replicating the finding of preserved associative spatial memory from our first experiment.

However, when first choice accuracy was examined in terms of starting position, *GluN1*$^{\Delta DGCA1}$ mice were impaired at choosing the correct beacon when started from close to the incorrect/decoy beacon (S^-), but not when starting from either of the other start locations (S^+ or equidistant; Fig. 6e). Not surprisingly, given that they had learned to swim towards the beacon as a means of escape during pre-training, all mice initially approached the first beacon that they encountered which resulted in sub-chance performance on S^- trials and above-chance performance on S^+ trials. Mice then gradually learned to inhibit this approach response depending on the spatial location of the beacon. ANOVA of first choice accuracy also revealed a main effect of start position, which was due to poorer performance when mice started close to the S^- beacon and better performance when they started close to the S^+ position ($F(2,42) = 233.50$; $p < 0.0001$). There was also a significant genotype by start position interaction ($F(2,42) = 4.24$; $p < 0.025$). Further investigation, using analysis of simple main effects, confirmed that *GluN1*$^{\Delta DGCA1}$ mice were impaired when trials started from close to the S^- beacon ($F(1,21) = 5.92$; $p < 0.025$), but not when trials started close to the S^+ beacon ($F < 1$; $p > 0.80$), nor from equidistant between the beacons ($F(1,21) = 1.86$; $p > 0.10$). Separate ANOVAs revealed significant improvements with training for each start position (main effect of block; S^- trials - $F(4,84) = 8.24$; $p < 0.0001$; equidistant trials - $F(4,84) = 24.50$; $p < 0.0001$; S^+ trials - $F(4,84) = 5.63$; $p < 0.0005$). Importantly, by the end of training, the control mice were exhibiting above chance levels of performance from all start positions (e.g. S^- trials only; one group t-test - $p < 0.05$).

Because mice sometimes swam under the S^- beacon and then re-emerged before, again, swimming under the S^- beacon, we also analyzed total errors in which each repeated choice added to the cumulated score for the trial. This revealed a main effect of genotype ($F(1,21) = 18.53$; $p < 0.0005$) and an interaction between genotype and starting position ($F(2,42) = 5.18$; $p < 0.01$; Supplementary Fig. 8). Subsequent analysis of the genotype by start position interaction using simple main effects confirmed that *GluN1*$^{\Delta DGCA1}$ mice were impaired on S^- trials ($F(1,21) = 17.02$; $p < 0.001$), and unimpaired on S^+ trials ($F < 1$; $p > 0.30$). On the total errors measure they were now significantly impaired on equidistant trials as well ($F(1,21) = 5.39$; $p < 0.05$), presumably because if they did approach the wrong beacon they were then more likely than Controls to persist in that response.

Non-spatial discrimination using a beacon watermaze task

GluN1$^{\Delta DGCA1}$ mice performed as well as Controls on an analogous, non-spatial version of the task in which they had to choose between two visually distinctive beacons[27] (grey funnel vs. black/white striped cylinder; Fig. 7a,b). Mice acquired the visual discrimination task, displaying increased first choice accuracy for the S^+ beacon and reduced total errors as training proceeded, but there were no group differences (Fig. 7c,d, Supplementary Fig. 9). As in the spatial discrimination task, mice found the task harder (they were less accurate with their first choices and made more errors), when starting from close to the S^- beacon. Conversely, they performed more efficiently when trials started from close to the S^+ beacon. ANOVA of first choice accuracy revealed a main effect of block, demonstrating acquisition of the task ($F(5,75) = 27.80$; $p < 0.0001$; Fig. 7c). There was also a main effect of start position which was due to mice being more likely to choose incorrectly when starting from close to the S^- beacon, and more likely to choose correctly when starting from closer to the S^+ beacon ($F(2,30) = 48.20$; $p < 0.0001$; Fig. 7c right, 7d). Importantly, however, there was no main effect of genotype or significant interaction involving genotype (ANOVA; genotype - $F < 1$; $p > 0.60$; genotype by block, genotype by start position - both $F < 1$; $p > 0.60$; genotype by block by start position - $F(10,150) = 1.09$; $p > 0.30$). Similar results were

obtained when analyzing total errors (Supplementary Fig. 9). Finally, there was no impairment in *GluN1*$^{\Delta DGCA1}$ mice during subsequent reversal of the non-spatial beacon task (Supplementary Fig. 10).

DISCUSSION

The present results show that NMDARs on DG and dorsal CA1 principal cells are not essential neuronal underpinnings of hippocampus-dependent spatial memory acquisition or storage. Instead they may play a critical role in using spatial information to guide selection between alternative responses. Despite ablation of NMDARs from both DG granule cells and dorsal CA1 pyramidal cells, and additionally some DG granule cell loss, *GluN1*$^{\Delta DGCA1}$ mice still acquired the hippocampus-dependent, spatial reference memory version of the watermaze as well as Controls. This was despite the loss of NMDAR currents and LTP in dorsal CA1 pyramidal cells in these animals. Importantly, although our manipulation was not confined to dorsal CA1 but also affected ventral CA1 and the entire DG, these additional consequences cannot explain the lack of a deficit on the standard watermaze task. Furthermore, while there is a gradient in ventral hippocampus of residual CA1 pyramidal cells that retain NMDARs, it is unlikely that these could support watermaze acquisition because lesion data from both rats and mice show that this ventral region alone is insufficient to support spatial learning on this task[18-20].

In contrast, *GluN1*$^{\Delta DGCA1}$ mice were unable to acquire the hippocampus-dependent, spatial reference memory radial maze task. This dissociation between the two classic tests of associative long-term spatial memory is not due to different sensorimotor or motivational task demands, but instead reflects the different psychological processes involved. To investigate this dissociation further, a variant of the watermaze task was run in which mice were required to solve a spatial discrimination between two visually identical beacons. *GluN1*$^{\Delta DGCA1}$ mice were less able than Controls to withhold responding to the incorrect, decoy beacon despite an equal knowledge of the spatial location of the platform. This did not reflect a generalized increase in approach tendencies. When two visually distinct, and hence unambiguous, beacons were used, *GluN1*$^{\Delta DGCA1}$ mice were unimpaired. Thus, an account based on how likely mice were to swim to any beacon, or based on task difficulty, cannot explain these data. Instead the impairment in the spatial task arose specifically as a result of the ambiguity evoked from two identical beacons. While previous studies have revealed dissociations within the domain of associative, long-term spatial memory[29], here we show that even when spatial navigation is normal in *GluN1*$^{\Delta DGCA1}$ mice, they are unable to use that spatial knowledge to select appropriately between competing response options.

The behavioral consequences in *GluN1*$^{\Delta DGCA1}$ mice were distinct from those seen after NMDAR deletion restricted to just DG granule cells[14]. *GluN1*$^{\Delta DG}$ mice displayed normal long-term associative spatial reference memory on the radial maze (although they did exhibit spatial working memory impairments). *GluN1*$^{\Delta DGCA1}$ mice in the present study were impaired on the associative, long-term reference memory radial maze task, and one might therefore conclude that it is the gene ablation in CA1 pyramidal cells that is specifically responsible, although we cannot rule out a cumulative phenotype in DG and CA1. Nevertheless, the very selective behavioral impairments exhibited by *GluN1*$^{\Delta DGCA1}$ mice, combined with the preserved ability to learn the spatial location of the platform in the watermaze, provide key information about the algorithm being performed by the hippocampus.

Our data dispute previous claims that NMDARs in dorsal CA1 are essential for associative spatial memory formation in the watermaze[7], based on conditional GluN1 knockout via the

Europe PMC Funders Author Manuscripts

Tg29-1 transgenic mouse line, which was thought to be confined to dorsal CA1 pyramidal cells. Potential differences between the two studies include genetic background, temporal onset of the genetic deletion, the dorsal/ventral extent of GluN1 ablation within the hippocampus and the age of the animals. The most likely explanation, however, is the lack of hippocampal selectivity of the GluN1 gene knockout, which more recent studies of the *Tg29-1* line have demonstrated spreads into cortical areas[9-13]. Subsequent publications report a clear reduction in GluN1 levels, measured by *in situ* hybridisation and immunocytochemistry, as early as 2 months of age if not sooner[11, 13]. Indeed, the *Tg29-1* line expresses Cre in cortex as early as 6 weeks post-natally[9]. The evidence that Cre expression, and hence loss of NMDARs, occurs outside of the hippocampus with this transgenic line is now compelling (see also[10, 12]). Notably, the *Tg29-1* mice with floxed *Grin1* alleles were also impaired on a visually cued version of the watermaze paradigm[7], demonstrating a hippocampus-independent learning impairment and indicating an effect of GluN1 deletion outside the hippocampus.

Combined with our current data, these results suggest that NMDARs, either elsewhere in the extended hippocampal formation, such as entorhinal cortex[30] or subiculum[31], or across the wider cortical mantle, could underlie associative spatial memory performance in the watermaze. Notably, a similar conclusion arises from studies with GluN2B knockout mice. Whereas genetic deletion of the GluN2B subunit from both hippocampus and cortex impaired watermaze acquisition[12], deletion of the subunit specifically from dorsal CA1 pyramidal cells and DG granule cells had no effect on acquisition[22]. Thus, there is likely to be an important role for cortical NMDARs in spatial memory acquisition.

At first glance the current results also appear at odds with pharmacological studies in rats. Intracerebroventricular infusion of the NMDAR antagonist AP5 impaired acquisition of the reference memory version of the watermaze[4]. Of course, intracerebroventricular infusion will affect both hippocampal and extra-hippocampal NMDARs. Even so, subsequent experiments found that watermaze acquisition was not impaired by NMDAR blockade using AP5 if rats had first been pre-trained as normal animals on a spatial task in a different laboratory[5, 6]. This is consistent with the present data in demonstrating that hippocampal NMDARs are not necessary (i) for spatial navigation per se, nor (ii) for forming a long-term association between a particular spatial location and the platform. In a further parallel with *GluN1*$^{\Delta DGCA1}$ mice in the present study, despite spatial pre-training, AP5 treated rats were impaired during spatial reversal in the watermaze when the location of the platform was switched to a novel place within the same, familiar environment[32].

Thus, the role of hippocampal NMDARs lies not in associative memory formation but elsewhere. Although NMDAR deletion in DG and dorsal CA1 principal cells does not prevent encoding of long-term spatial memories, it does affect the use of spatial information to disambiguate between overlapping or competing associative memories. It has been suggested that the hippocampus is a key component of a comparator system to detect mismatch or conflict[33, 34]. Human fMRI experiments[35-37] and both electrophysiological unit recording[38-40] and lesion studies[41] in rodents have implicated the hippocampus, and particularly the CA1 subfield, with a role in detecting and/or resolving associative mismatch and conflict, such as might occur between an expectation based on information retrieved from long-term memory and the current state of the perceptual world. This comparator function is not, however, a reward prediction error signal that determines the extent of associative learning[42]. Instead, one key output of this hippocampal mismatch detection system is behavioral inhibition of on-going activity[33, 34], modifying within-trial performance without affecting the progressive changes in associative learning from trial to trial. A failure in this process likely underlies the deficit in *GluN1*$^{\Delta DGCA1}$ mice when the platform was moved to the opposite quadrant of the pool during the first watermaze

experiment (Fig. 3a, **Reversal**; see also[32]). Notably, *GluN1*$^{\Delta DGCA1}$ mice were not impaired in either of two non-spatial reversal paradigms. This excludes an account based on a general tendency to perseverate all learned responses.

The present results also demonstrate a novel but related role for hippocampal NMDARs in resolving interference between competing long-term memories, so enabling behavioral inhibition of inappropriately cued or conditioned responses on the basis of spatial or contextual information. This key deficit in *GluN1*$^{\Delta DGCA1}$ mice manifested as an inability to withhold responding to the decoy beacon, despite knowing the spatial location of the platform. Critically, this did not reflect a general inability to inhibit all approach responses, as evidenced by the normal performance of *GluN1*$^{\Delta DGCA1}$ mice on the visual discrimination beacon task, irrespective of start position. Instead, the deficit occurred when a conflict arose as the result of ambiguity between competing long-term memories associated with two visibly identical beacons. This same account can explain the radial maze deficit in *GluN1*$^{\Delta DGCA1}$ mice, which results from the ambiguity that arises from the identical physical appearance of all 6 arms of the maze.

It has repeatedly been suggested that an important role of the hippocampus is pattern separation to disambiguate between overlapping inputs[43-45]. On this occasion the ambiguity arises, not from overlapping extramaze spatial cues, but from the similarity of the maze arms or the visibly identical beacons, and the fact that these cues are associated with conflicting outcomes. Thus, at a psychological level, NMDARs in the hippocampus may serve to resolve conflict or ambiguity as a result of detecting mismatch or uncertainty rather than sub-serving learning by detecting coincidence.

Supplementary Material

Refer to Web version on PubMed Central for supplementary material.

Acknowledgments

We thank Ulla Amtmann, Hannah Monyer and Illaria Bertocchi for *in situ* hybridization and Wanan Tang and Daria Arcos Diaz for rAAV injections. We thank Rob Deacon for assistance with lesion surgeries. This work was supported by a grant from the European Commission to the EUSynapse project (LSHM-CT-2005-019055) to PHS, Wellcome Trust SRFs 074385 and 087736 to DMB, a grant from the German Research Foundation SFB636/A4; BMFT:NGFN/SP10, DFG-GA 427/8-1 to RS and the Bauer-Stiftung to T.B. ØH and VJ were supported by the Letten Foundation.

References

1. Bliss TV, Collingridge GL. A synaptic model of memory: long-term potentiation in the hippocampus. Nature. 1993; 361:31–9. [PubMed: 8421494]
2. Martin SJ, Grimwood PD, Morris RG. Synaptic plasticity and memory: an evaluation of the hypothesis. Annu. Rev. Neurosci. 2000; 23:649–711. [PubMed: 10845078]
3. Neves G, Cooke SF, Bliss TV. Synaptic plasticity, memory and the hippocampus: a neural network approach to causality. Nat. Rev. Neurosci. 2008; 9:65–75. [PubMed: 18094707]
4. Morris RG, Anderson E, Lynch GS, Baudry M. Selective impairment of learning and blockade of long-term potentiation by an N-methyl-D-aspartate receptor antagonist, AP5. Nature. 1986; 319:774–776. [PubMed: 2869411]
5. Bannerman DM, Good MA, Butcher SP, Ramsay M, Morris RG. Distinct components of spatial learning revealed by prior training and NMDA receptor blockade. Nature. 1995; 378:182–186. [PubMed: 7477320]
6. Saucier D, Cain DP. Spatial learning without NMDA receptor-dependent long-term potentiation. Nature. 1995; 378:186–189. [PubMed: 7477321]

7. Tsien JZ, Huerta PT, Tonegawa S. The essential role of hippocampal CA1 NMDA receptor-dependent synaptic plasticity in spatial memory. Cell. 1996; 87:1327–1338. [PubMed: 8980238]
8. Tsien JZ, et al. Subregion- and cell type-restricted gene knockout in mouse brain. Cell. 1996; 87:1317–1326. [PubMed: 8980237]
9. Wiltgen BJ, et al. A role for calcium-permeable AMPA receptors in synaptic plasticity and learning. PLoS One. 2010; 5:e12818. [PubMed: 20927382]
10. Hoeffer CA, et al. Removal of FKBP12 enhances mTOR-Raptor interactions, LTP, memory, and perseverative/repetitive behavior. Neuron. 2008; 60:832–845. [PubMed: 19081378]
11. Fukaya M, Kato A, Lovett C, Tonegawa S, Watanabe M. Retention of NMDA receptor NR2 subunits in the lumen of endoplasmic reticulum in targeted NR1 knockout mice. Proc. Natl. Acad. Sci. USA. 2003; 100:4855–4860. [PubMed: 12676993]
12. Brigman JL, et al. Loss of GluN2B-containing NMDA receptors in CA1 hippocampus and cortex impairs long-term depression, reduces dendritic spine density, and disrupts learning. J. Neurosci. 2010; 30:4590–4600. [PubMed: 20357110]
13. Rondi-Reig L, et al. Impaired sequential egocentric and allocentric memories in forebrain-specific-NMDA receptor knock-out mice during a new task dissociating strategies of navigation. J. Neurosci. 2006; 26:4071–4081. [PubMed: 16611824]
14. Niewoehner B, et al. Impaired spatial working memory but spared spatial reference memory following functional loss of NMDA receptors in the dentate gyrus. Eur. J. Neurosci. 2007; 25:837–846. [PubMed: 17313573]
15. McHugh TJ, et al. Dentate gyrus NMDA receptors mediate rapid pattern separation in the hippocampal network. Science. 2007; 317:94–99. [PubMed: 17556551]
16. Murray AJ, et al. Parvalbumin-positive CA1 interneurons are required for spatial working but not for reference memory. Nat. Neurosci. 2011; 14:297–9. [PubMed: 21278730]
17. Dillon GM, Qu X, Marcus JN, Dodart JC. Excitotoxic lesions restricted to the dorsal CA1 field of the hippocampus impair spatial memory and extinction learning in C57BL/6 mice. Neurobiol. Learn. Mem. 2008; 90:426–433. [PubMed: 18602845]
18. Logue SF, Paylor R, Wehner JM. Hippocampal lesions cause learning deficits in inbred mice in the Morris water maze and conditioned-fear task. Behav. Neurosci. 1997; 111:104–113. [PubMed: 9109628]
19. Bannerman DM, et al. Double dissociation of function within the hippocampus: a comparison of dorsal, ventral, and complete hippocampal cytotoxic lesions. Behav. Neurosci. 1999; 113:1170–1188. [PubMed: 10636297]
20. Moser MB, Moser EI, Forrest E, Andersen P, Morris RG. Spatial learning with a minislab in the dorsal hippocampus. Proc. Natl. Acad. Sci USA. 1995; 92:9697–9701. [PubMed: 7568200]
21. Pothuizen HH, Zhang WN, Jongen-Relo AL, Feldon J, Yee BK. Dissociation of function between the dorsal and the ventral hippocampus in spatial learning abilities of the rat: a within-subject, within-task comparison of reference and working spatial memory. Eur. J. Neurosci. 2004; 19:705–712. [PubMed: 14984421]
22. von Engelhardt J, et al. Contribution of hippocampal and extra-hippocampal NR2B-containing NMDA receptors to performance on spatial learning tasks. Neuron. 2008; 60:846–860. [PubMed: 19081379]
23. Shimshek DR, et al. Enhanced odor discrimination and impaired olfactory memory by spatially controlled switch of AMPA receptors. PLoS Biol. 2005; 3:e354. [PubMed: 16216087]
24. Suchanek B, Seeburg PH, Sprengel R. Tissue specific control regions of the N-methyl-D-aspartate receptor subunit NR2C promoter. Biol. Chem. 1997; 378:929–934. [PubMed: 9377491]
25. Tashiro A, Sandler VM, Toni N, Zhao C, Gage FH. NMDA-receptor-mediated, cell-specific integration of new neurons in adult dentate gyrus. Nature. 2006; 442:929–933. [PubMed: 16906136]
26. Lyon L, et al. Fractionation of spatial memory in GRM2/3 (mGlu2/mGlu3) double knockout mice reveals a role for group II metabotropic glutamate receptors at the interface between arousal and cognition. Neuropsychopharmacology. 2011; 36:2616–2628. [PubMed: 21832989]

27. Morris RG, Hagan JJ, Rawlins JN. Allocentric spatial learning by hippocampectomised rats: a further test of the “spatial mapping” and “working memory” theories of hippocampal function. Q. J. Exp. Psychol. B. 1986; 38:365–95. [PubMed: 3809580]
28. Uekita T, Okaichi H. Pretraining does not ameliorate spatial learning deficits induced by intrahippocampal infusion of AP5. Behav. Neurosci. 2009; 123:520–526. [PubMed: 19485557]
29. Brun VH, et al. Place cells and place recognition maintained by direct entorhinal-hippocampal circuitry. Science. 2002; 296:2243–2246. [PubMed: 12077421]
30. Steffenach HA, Witter M, Moser MB, Moser EI. Spatial memory in the rat requires the dorsolateral band of the entorhinal cortex. Neuron. 2005; 45:301–313. [PubMed: 15664181]
31. Morris RG, Schenk F, Tweedie F, Jarrard LE. Ibotenate Lesions of Hippocampus and/or Subiculum: Dissociating Components of Allocentric Spatial Learning. Eur. J. Neurosci. 1990; 2:1016–1028. [PubMed: 12106063]
32. Morris RG, Davis S, Butcher SP. Hippocampal synaptic plasticity and NMDA receptors: a role in information storage? Philos Trans. R. Soc. Lond. B. Biol. Sci. 1990; 329:187–204. [PubMed: 1978364]
33. Vinogradova, OS. The Hippocampus. Pribram, RIIKH., editor. Plenum Press; New York: 1975. p. 3-69.
34. Gray, JA.; McNaughton, N. The Neuropsychology of Anxiety. Oxford University Press; Oxford: 2000.
35. Ploghaus A, et al. Learning about pain: the neural substrate of the prediction error for aversive events. Proc. Natl. Acad. Sci. USA. 2000; 97:9281–9286. [PubMed: 10908676]
36. Kumaran D, Maguire EA. Match mismatch processes underlie human hippocampal responses to associative novelty. J. Neurosci. 2007; 27:8517–8524. [PubMed: 17687029]
37. Kumaran D, Maguire EA. An unexpected sequence of events: mismatch detection in the human hippocampus. PLoS Biol. 2006; 4:e424. [PubMed: 17132050]
38. O’Keefe, J.; Nadel, L. The hippocampus as a cognitive map. Clarendon Press; Oxford: 1978. Oxford
39. O’Keefe J. Place units in the hippocampus of the freely moving rat. Exp. Neurol. 1976; 51:78–109. [PubMed: 1261644]
40. Fyhn M, Molden S, Hollup S, Moser MB, Moser E. Hippocampal neurons responding to first-time dislocation of a target object. Neuron. 2002; 35:555–566. [PubMed: 12165476]
41. Honey RC, Watt A, Good M. Hippocampal lesions disrupt an associative mismatch process. J. Neurosci. 1998; 18:2226–2230. [PubMed: 9482806]
42. Hollerman JR, Schultz W. Dopamine neurons report an error in the temporal prediction of reward during learning. Nat. Neurosci. 1998; 1:304–309. [PubMed: 10195164]
43. Marr D. Simple memory: a theory for archicortex. Philos. Trans. R. Soc. Lond. B. Biol. Sci. 1971; 262:23–81. [PubMed: 4399412]
44. Rolls, ETT.; A.. Neural networks and brain function. OUP; Oxford: 1998.
45. Sahay A, Wilson DA, Hen R. Pattern separation: a common function for new neurons in hippocampus and olfactory bulb. Neuron. 70:582–588. [PubMed: 21609817]
46. Lee G, Saito I. Role of nucleotide sequences of loxP spacer region in Cre-mediated recombination. Gene. 1998; 216:55–65. [PubMed: 9714735]
47. Soriano P. Generalized lacZ expression with the ROSA26 Cre reporter strain. Nat. Genet. 1999; 21:70–71. [PubMed: 9916792]
48. Jerecic J, et al. Impaired NMDA receptor function in mouse olfactory bulb neurons by tetracycline-sensitive NR1 (N598R) expression. Brain. Res. Mol. Brain. Res. 2001; 94:96–104. [PubMed: 11597769]
49. Krestel HE, Mayford M, Seeburg PH, Sprengel R. A GFP-equipped bidirectional expression module well suited for monitoring tetracycline-regulated gene expression in mouse. Nucleic Acids Res. 2001; 29:E39. [PubMed: 11266574]
50. Jensen V, et al. A juvenile form of postsynaptic hippocampal long-term potentiation in mice deficient for the AMPA receptor subunit GluR-A. J. Physiol. 2003; 553:843–856. [PubMed: 14555717]

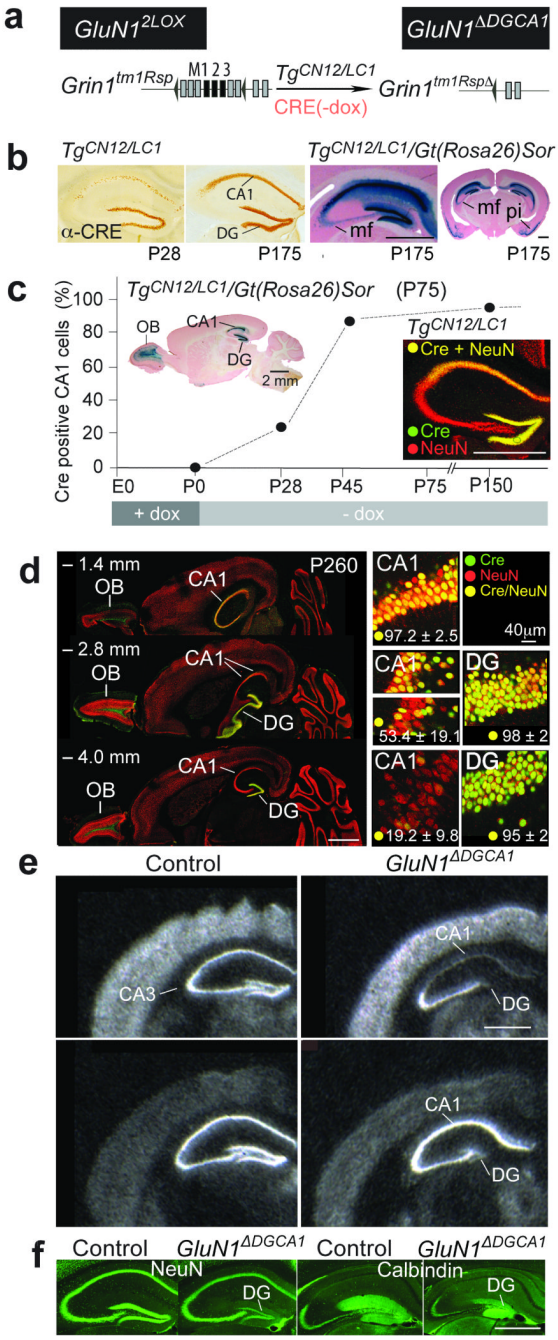

Figure 1. Removal of NMDARs in DG and CA1

(a) Genes to generate conditional *NMDAR*$^{-/-}$ mice (*GluN1*$^{\Delta DGCA1}$) by postnatal dox-controlled activation of *Tg*$^{CN12/LC1}$-encoded Cre in *Grin1*^{tm1Rsp} mice (*GluN1*^{2lox}). LoxP sites are depicted by black triangles. Exons appear as boxes, and when black, encode membrane-spanning segments. **(b)** Anti-Cre immunostainings of brain sections from dox treated (till P0) *Tg*$^{CN12/LC1}$ mice at postnatal days P28 and P175, and β-galactosidase stainings (blue) of sections from *Tg*$^{CN12/LC1}$*/Gt(Rosa)26Sor* mice (mf, mossy fibers; pi, piriform cortex with ~30% of layer II neurons expressing Cre). (**c, d**) Dox-regulated Cre expression in the brains of *Tg*$^{CN12/LC1}$ mice. (**c**) Expression pattern of the nuclearly

localized Cre in CA1 pyramidal cells when dox had been removed from the drinking water of mothers at the day of delivery. At P28 (n=2 mice), P45 (n=2) and P150 (n=6), the extent of Cre expressing pyramidal neurons in the dorsal CA1 layer was estimated by α-Cre immunostains (green), counterstained with α-NeuN (red). The inset shows Cre-activated β-galactosidase expression in CA1 and DG of the hippocampus and the olfactory bulb (OB) in a brain section from $Tg^{CN12/LC1}/Gt(Rosa)26Sor$ mice. (**d, left**), Horizontal brain sections of $Tg^{CN12/LC1}$ mice immunostained with α-Cre (green) and α-NeuN (red) at three different levels from bregma (– 1.4, – 2.8, and – 4.0 mm) showed a yellow gradient of Cre/NeuN immunoreactivity in the dorsal to ventral str. pyramidale of CA1, but not in the DG. The percentage of Cre positive cells among >1,000 NeuN positive neurons was evaluated at various depths in dorsal and ventral hippocampus, in slices from four P260 $GluN1^{\Delta DGCA1}$ mice, and is listed as mean ± SD. (**d, right**) High magnification examples of α-Cre/α-NeuN co-labeled CA1 and DG neurons (yellow) from sections given on the left. The transition between dorsal and ventral hippocampus in the rostro-caudal axis had the highest variance of Cre expressing NeuN positive cells (middle insets). Other parts of the hippocampal formation feature negligible numbers of Cre-positive cells (<1% co-labeling). (**e**) *In situ* hybridization with GluN1 and GluA1 probes. Scale bars, 2mm. **(f)** α-NeuN and α-Calbindin immunostainings.

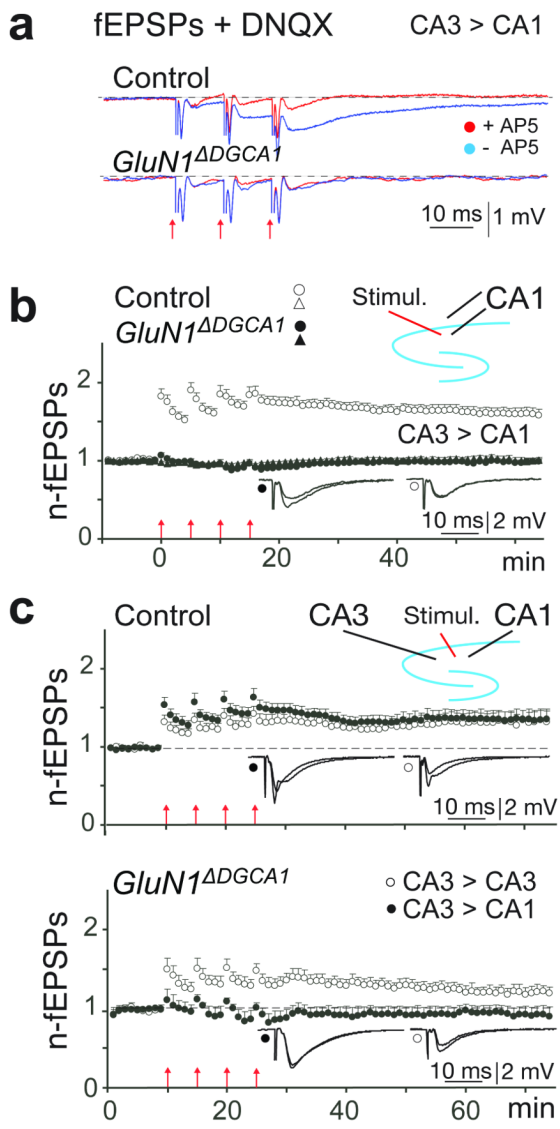

Figure 2. Loss of functional NMDA receptors at CA3-to-CA1 synapses in the dorsal CA1 region

(a) Absence of NMDA responses in field recordings in acute brain slices from 10 to 12 month old *GluN1*$^{\Delta DGCA1}$ mice: Blue traces show the average (five repetitions at 0.1 Hz) of fEPSPs elicited by three synaptic activations at 100 Hz in the presence of the AMPA receptor blocker DNQX (20μM) in control (upper panel) and *GluN1*$^{\Delta DGCA1}$ (lower panel) mice. Red traces are the corresponding responses following subsequent superfusion with AP5 (50μM) to block NMDA receptors. Mean representative traces (averaged across 5 stimulations both before and after AP5) from a single slice from both a control and a *GluN1*$^{\Delta DGCA1}$ mouse. Experiments were repeated in 3 control (n=12 slices) and 2 *GluN1*$^{\Delta DGCA1}$ mice (n=8 slices). **(b) Absence of LTP:** Normalized and pooled fEPSP slopes evoked at CA1 radiatum and oriens synapses in slices from both control (open symbols) and *GluN1*$^{\Delta DGCA1}$ mice (filled symbols). Forty to 45 min after the last tetanization of the afferent fibres in the stratum radiatum in slices from five Controls, the average slope of the field EPSP (open circles) was 1.60 ± 0.07 (mean ± SEM; n=18 slices) of the pre-tetanic value, whereas the untetanized oriens pathway (triangles) was unchanged (0.97 ± 0.04). In slices from four *GluN1*$^{\Delta DGCA1}$ mice LTP was completely abolished (0.99

± 0.03, n=14 slices), and evoked responses were not significantly different from those in the untetanized pathway (1.03 ± 0.04; p = 0.35). **(c)** LTP at CA3-CA3 and CA3-CA1 synapses: normalized and pooled fEPSPs before and after LTP induction at CA3-CA3 (open circles) and CA3-CA1 (filled circles) radiatum synapses. In slices from three control mice (upper panel), LTP was well-developed 40 – 45 min post-tetanization, with similar magnitudes in the two regions (CA3; 1.33 ± 0.12, CA1; 1.37 ± 0.11; n=11 slices; p = 0.77). The same experimental paradigm performed on slices from three $GluN1^{\Delta DGCA1}$ mice (lower panel) showed preserved LTP in CA3 whereas LTP in CA1 failed to develop (CA3; 1.20 ± 0.07, CA1: 0.94 ± 0.19; n=8 slices; p = 0.01). All means ± s.e.m. Arrows at the abscissa indicate the time points of tetanic stimulation. Insets show means of six consecutive synaptic responses in the tetanized pathway before and 45 min post-tetanization.

Europe PMC Funders Author Manuscripts

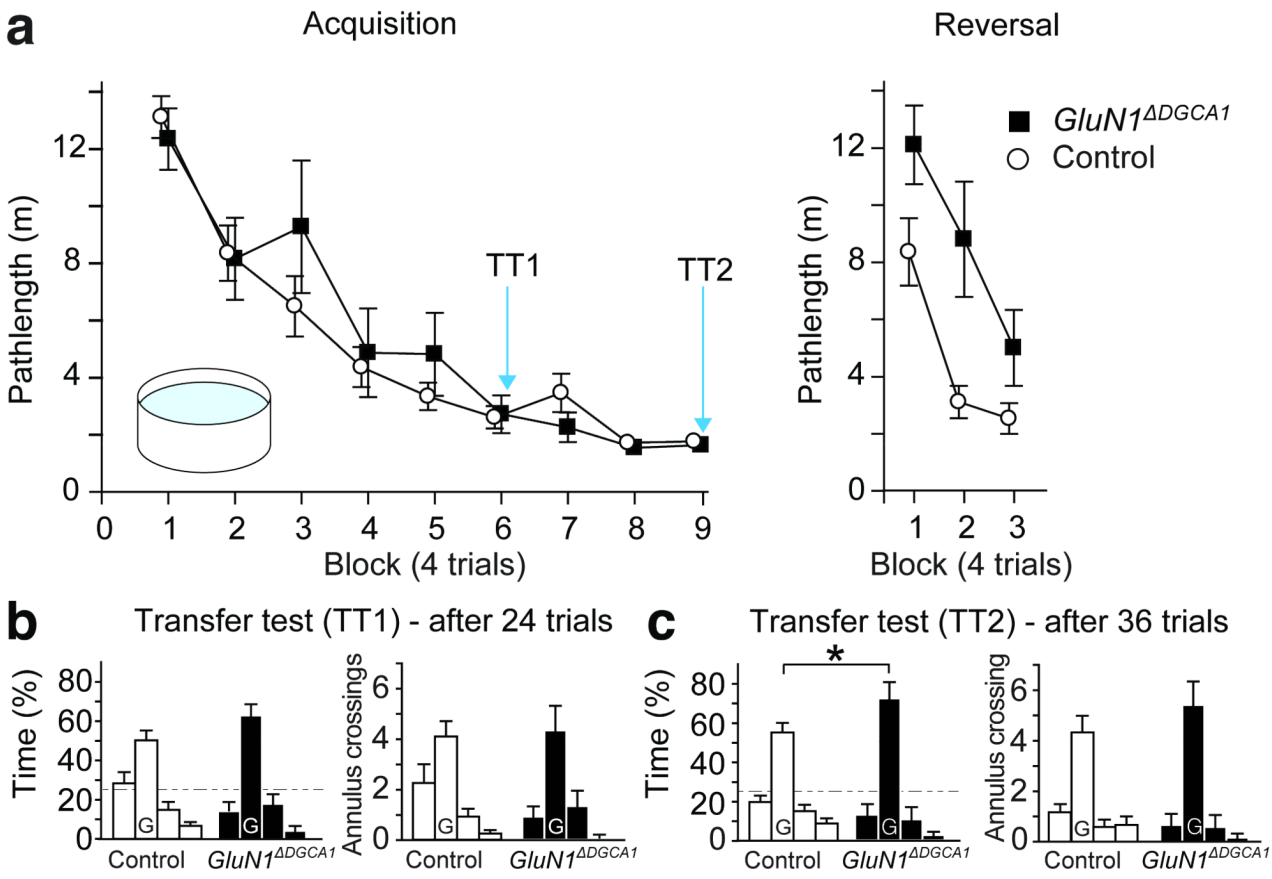

Figure 3. Associative long-term spatial reference memory in the Morris watermaze

(a) Similar pathlengths for Controls (n=12) and *GluN1*$^{\Delta DGCA1}$ mice (n=12) during Acquisition of the fixed location, hidden escape platform watermaze task (Acquisition; *geno* – F<1, *geno x block* – F(8,176)=1.64; p>0.10; 4 trials/block). When the platform was moved to the opposite quadrant of the pool (Reversal), the pathlengths of *GluN1*$^{\Delta DGCA1}$ mice were significantly longer than Controls (*geno* – F(1,22)=13.41; p<0.005). All means ± s.e.m. **(b, c)** Long-term memory performance during probe trials (Transfer tests) after 6 and 9 training blocks. Percentage time spent (left panel) and numbers of annulus crossings (right panel) in each quadrant (left to right; adjacent left, goal (G), adjacent right, opposite) for Controls and *GluN1*$^{\Delta DGCA1}$ mice. In transfer test 2 (TT2), *GluN1*$^{\Delta DGCA1}$ mice searched longer in the training quadrant than Controls (t(22)=2.24; * p<0.05). Broken line: chance levels of performance. In addition, the numbers of annulus crossings in each quadrant are given.

Europe PMC Funders Author Manuscripts

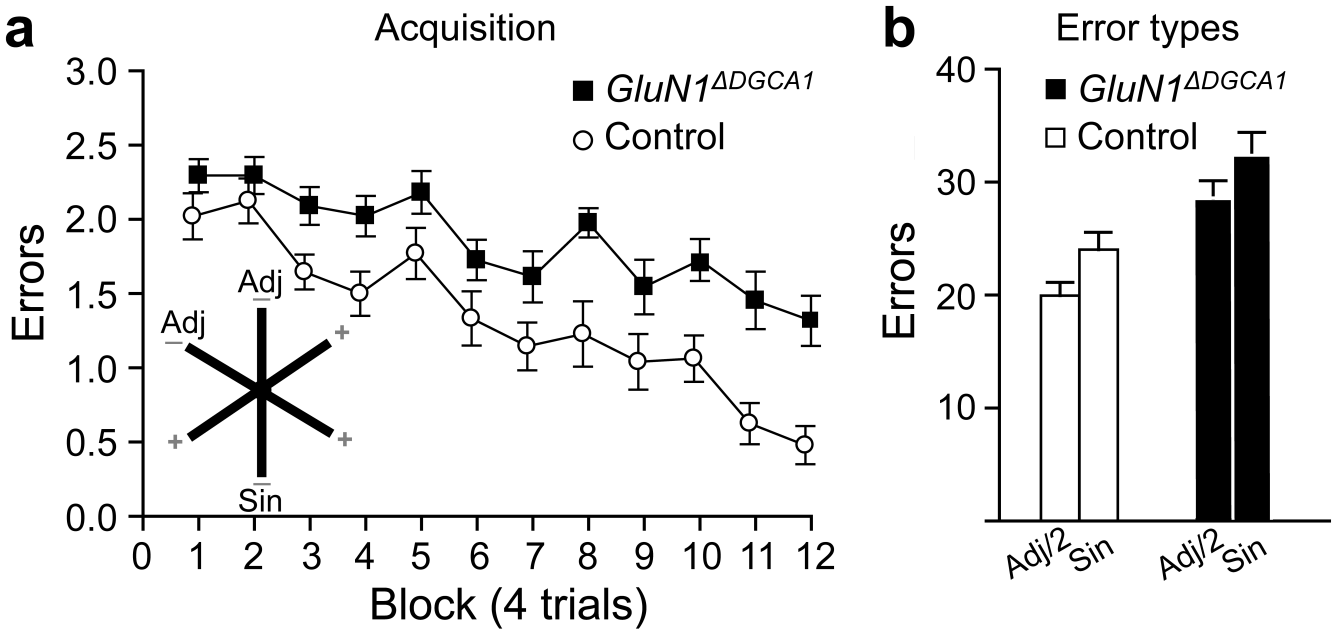

Figure 4. Associative long-term spatial reference memory on the radial maze task

(a) Inset: Mice were trained to discriminate between three rewarded (+) and three un-baited (−) arms. Errors per trial for Controls (n=12) and *GluN1*$^{\Delta DGCA1}$ mice (n=11) across 12 blocks of testing (4 trials per block). *GluN1*$^{\Delta DGCA1}$ mice were impaired at discriminating between the baited and non-baited arms, making significantly more spatial reference memory errors ($F(1,21) = 30.42$; $p<0.0001$). **(b)** Error types during spatial reference memory acquisition. Total number of errors into the single, non-rewarded arm (Sin) and the total number of errors into the pair of adjacent (Adj/2), non-rewarded arms. The number of errors into the pair of adjacent, un-baited arms was divided by two to correct for the number of arms. All means ± s.e.m.

Europe PMC Funders Author Manuscripts

Europe PMC Funders Author Manuscripts

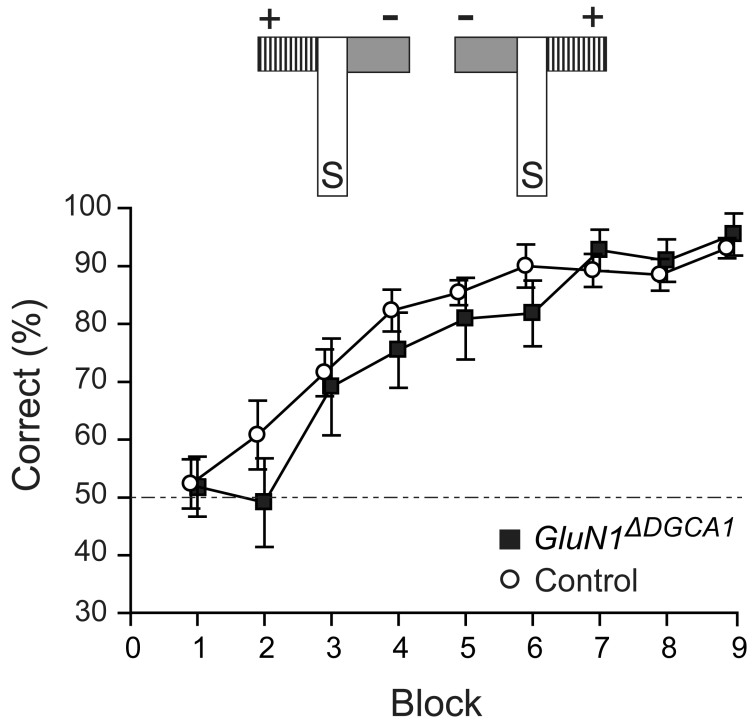

Figure 5. Preserved visual discrimination learning in *GluN1*$^{\Delta DGCA1}$ mice

In the visual discrimination task both Controls (n=13) and *GluN1*$^{\Delta DGCA1}$ mice (n=11) learned to associate floor/wall color (grey vs. black/white stripes) with a reward (+) independent of its spatial position in the arms of the maze. The top part of the figure depicts the T-maze with the start arm (S) and both the rewarded (+) and non-rewarded (−) goal arms, which can be arranged in either of two possible configurations. There were 9 blocks of training (10 trials per block). Mean ± s.e.m. percent correct choices for Controls and *GluN1*$^{\Delta DGCA1}$ mice. Broken line: chance levels of performance.

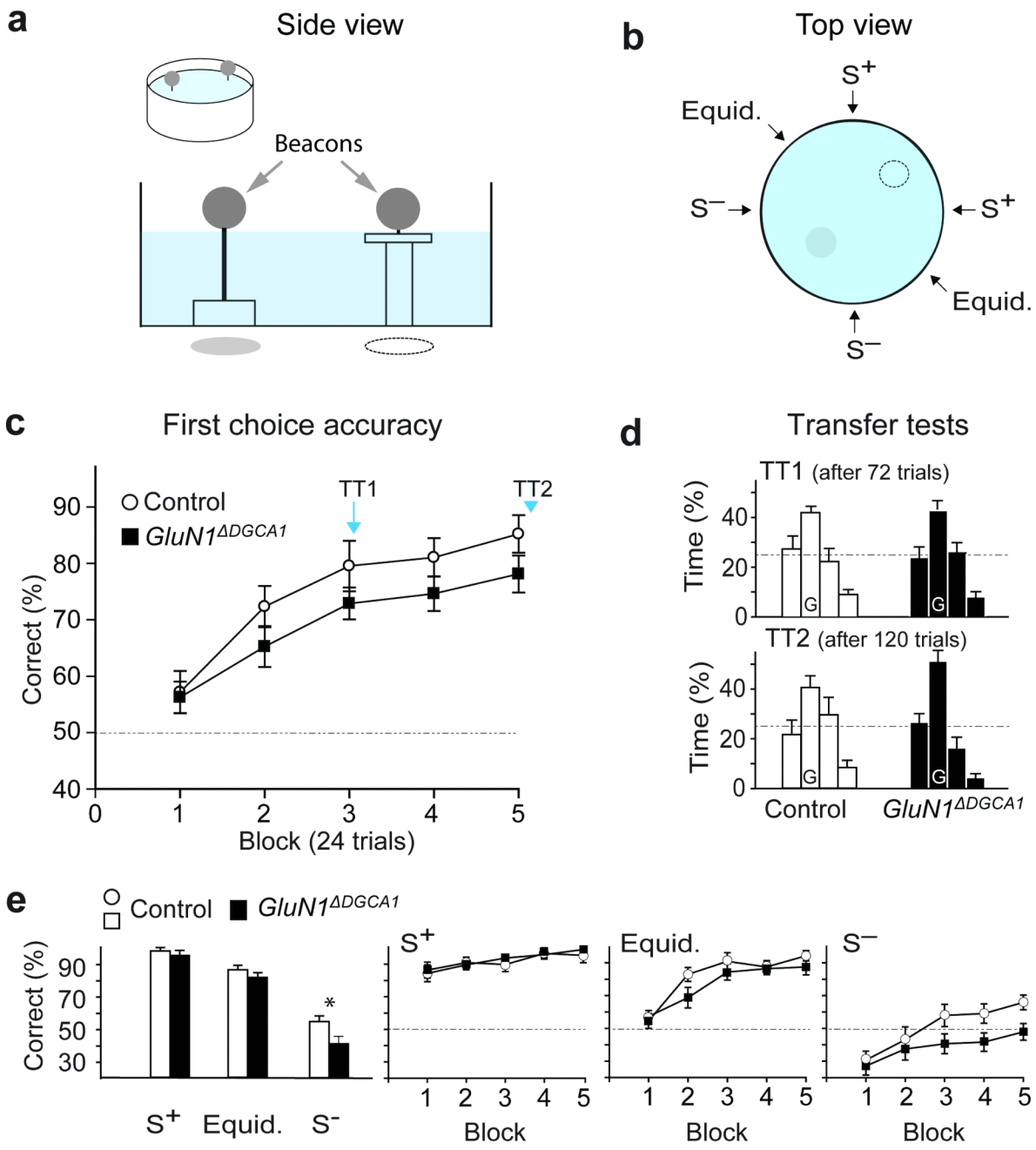

Figure 6. Spatial memory and choice performance on the spatial discrimination beacon watermaze task

(a) Schema and horizontal side view of the spatial beacon watermaze task. **(b)** Top view indicating the six possible start sites and the positions of the beacons (broken line = + Platform; shaded circle = – platform). **(c)** Both Controls (n=11) and *GluN1*$^{\Delta DGCA1}$ mice (n=12) learned to choose the correct beacon in terms of first choice accuracy: *geno* – F(1,21)=2.88; p>0.10, *geno x blocks* – F<1; 24 trials/block). **(d)** When probe tests (TT1 and TT2; beacons and platform removed) were conducted, both groups showed a strong preference for the goal quadrant (adjacent left, goal (G), adjacent right, opposite). **(e)** *GluN1*$^{\Delta DGCA1}$ mice were impaired at choosing the correct beacon when starting from a

Europe PMC Funders Author Manuscripts

point close to the incorrect beacon (S^-), but not when starting from either of the other two start locations; (S^+) or equidistant; *geno x start position* - $F(2,42)=4.24$; $p<0.025$, simple main effects group difference *$p<0.025$). **(e, right)** Mean ± s.e.m. percent correct choices across 5 blocks of training (8 trials/block) on trials starting from the S^+, the equidistant and the S^- position. Broken line, chance levels of performance. All means ± s.e.m.

Europe PMC Funders Author Manuscripts

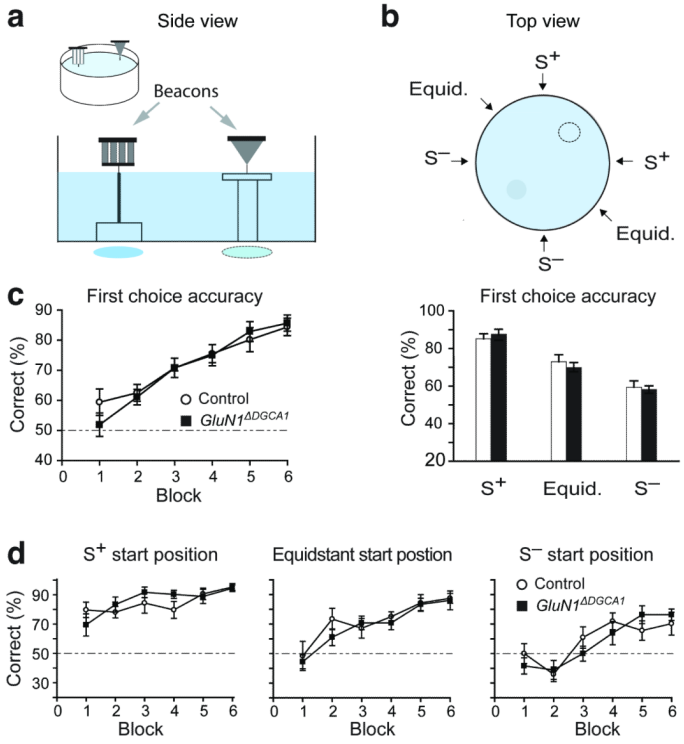

Figure 7. Normal performance of *GluN1*$^{\Delta DGCA1}$ mice on the visual discrimination beacon watermaze task

(a) Horizontal side view of the non-spatial beacon watermaze task. **(b)** Top view of the six possible start positions. **(c)** Both Controls (n=8) and *GluN1*$^{\Delta DGCA1}$ mice (n=9) learned to choose the correct beacon. First choice accuracy improved with training for both groups across 6 blocks of training (24 trials/block; **c, left**). The first choice accuracy across all training trials from different starting positions showed that all mice were less accurate at choosing the correct beacon when starting from S$^-$ (**c, right**). **(d)** Performance across 6 blocks of training on trials starting from S$^+$, equidistant and S$^-$ positions. All mice performed less accurately when starting from S$^-$. There was no difference between Controls and *GluN1*$^{\Delta DGCA1}$ mice across 6 blocks of training for any of the start positions (8 trials/block). Broken line: chance levels of performance. All means ± s.e.m.

Europe PMC Funders Author Manuscripts